

Manifest causality in quantum field theory with sources and detectors

Robert Dickinson,^a Jeff Forshaw,^a Peter Millington,^{a,b} and Brian Cox^c

^a*Consortium for Fundamental Physics, School of Physics & Astronomy,
University of Manchester, Manchester M13 9PL. U.K.*

^b*Institute for Particle Physics Phenomenology, Durham University,
Durham DH1 3LE. U.K.*

^c*School of Physics & Astronomy, University of Manchester,
Manchester M13 9PL. U.K.*

E-mail: robert.dickinson@hep.manchester.ac.uk,
jeff.forshaw@manchester.ac.uk,
peter.millington@hep.manchester.ac.uk,
brian.cox@hep.manchester.ac.uk

ABSTRACT: We introduce a way to compute scattering amplitudes in quantum field theory including the effects of particle production and detection. Our amplitudes are manifestly causal, by which we mean that the source and detector are always linked by a connected chain of retarded propagators. We show how these amplitudes can be derived from a path integral, using the Schwinger-Keldysh “in-in” formalism. Focussing on ϕ^3 theory, we confirm that our approach agrees with the standard S-matrix approach in the case of positive energy plane-wave scattering.

KEYWORDS: Quantum Field Theory, Thermal Field Theory

ARXIV EPRINT: [1312.3871](https://arxiv.org/abs/1312.3871)

Contents

1	Introduction	1
2	Expectation values of local operators	2
3	Scattering amplitudes	6
4	Path integral representation	10
5	Relation to S-matrix	15
A	Relation to unitarity cutting rules	18
B	Propagator definitions	22

1 Introduction

Although relativistic quantum field theories are built with causality in mind, the way causality plays out at the level of the particle dynamics is not so clear. The usual “in-out” formalism places production and detection sources on the same footing and amplitudes involve only the Feynman propagator. Our approach replaces the usual expression for the scattering matrix by an “in-in” expectation value in which detection is distinct from production. It leads to manifestly causal results, in which the retarded propagator is prominent.

In section 2 we begin by presenting a general result for the expectation value of a hermitian operator that is some local function of field operators; we have in mind that the operator represents an observable. We do this in the presence of an external source and show that the effect of the source is transmitted to the detector via an unbroken chain of retarded propagators. Feynman propagators necessarily appear but never so as to break the causal link from source to detector.

In section 3 we present an expression for the calculation of scattering amplitudes. Since these can be expressed as expectation values of non-local products of field operators, we can use many of the results of the previous section. We then present the corresponding Feynman rules and illustrate their use in tree-level scattering.

In section 4 we show that our scattering amplitudes can be derived from a path integral in the “in-in” formalism. In section 5, we prove the equivalence of our scattering amplitudes, in the case of positive energy plane-wave scattering, with those obtained from the S-matrix. In appendix A, we describe the link with the cutting rules of thermal field theory.

2 Expectation values of local operators

We shall consider a single real scalar field, $\phi_x \equiv \phi(x)$, in the presence of some external disturbance that is active within a spacetime region \mathcal{R}_J . We suppose that a measurement taking place within a spacetime region \mathcal{R}_B is represented by a hermitian operator B that is some function of the field operator within the region, i.e. $B \equiv B(\{\phi_x : x \in \mathcal{R}_B\})$, and that the disturbance is represented by a contribution to the Hamiltonian of the form

$$\int_{\mathcal{R}_J} d^4x \gamma \mathcal{J}(\phi_x, x) .$$

Given a source whose strength is parametrised by γ , the sensitivity σ_B of a detector making measurement B may be expressed as

$$\sigma_B = \frac{\partial}{\partial \gamma} \langle B \rangle . \quad (2.1)$$

In what follows, we will show that σ_B can be expressed using chains of retarded propagators from \mathcal{R}_J to \mathcal{R}_B , which implies that it vanishes outside of the forward light cone of the source.

In the interaction picture (which we always employ) the system evolves as

$$|\psi(t)\rangle = U(t, t_A) |\psi_A\rangle \quad (2.2)$$

where

$$\begin{aligned} U(t, t_A) = & 1 + (-i) \int_{t_A}^t dt_1 H_1 + (-i)^2 \int_{t_A}^t dt_1 dt_2 \Theta_{12} H_1 H_2 + \dots \\ & + (-i)^n \int_{t_A}^t dt_1 \dots dt_n \Theta_{1\dots n} H_1 \dots H_n + \dots , \end{aligned} \quad (2.3)$$

is the evolution operator and $\Theta_{ijk\dots} \equiv \Theta(t_i > t_j > t_k > \dots)$ is a Heaviside function, defined to be 1 if the time-ordered condition within the brackets is satisfied and 0 otherwise. $H_i \equiv H_{\text{int}}(t_i)$ is the interaction Hamiltonian, including the effect of the source.

The expectation value of an operator B at a given time t_0 may then be written as

$$\langle B \rangle_{t=t_0} = \langle \psi_A | U^\dagger(t_0, t_A) B(t_0) U(t_0, t_A) | \psi_A \rangle . \quad (2.4)$$

Rather than express $U(t, t_A)$ as a time-ordered exponential, we use a generalisation of the Baker–Hausdorff lemma [1], i.e. with $B_0 \equiv B(t_0)$ we write

$$U^\dagger(t_0, t_A) B_0 U(t_0, t_A) = F_0 + F_1 + F_2 + \dots \quad (2.5)$$

with each term expressed as a set of nested commutators:

$$\begin{aligned}
F_0 &= B_0 \\
F_1 &= (-i) \int_{t_A}^{t_0} dt_1 \Theta_{01} [B_0, H_1] \\
F_2 &= (-i)^2 \int_{t_A}^{t_0} dt_1 dt_2 \Theta_{012} [[B_0, H_1], H_2] \\
&\vdots \\
F_n &= (-i)^n \int_{t_A}^{t_0} dt_1 \dots dt_n \Theta_{01\dots n} \left[\dots \left[[[B_0, H_1], H_2], H_3 \right] \dots, H_n \right] \\
&\vdots
\end{aligned} \tag{2.6}$$

Note that within each integral, $t_0 > t_1 > \dots > t_n > t_A$. To encompass the full extent of the influence of the source, t_A must be a time prior to any point in \mathcal{R}_J .

For the expectation value of B , we have

$$\begin{aligned}
\langle B \rangle_{t=t_0} &= \sum_{n=0}^{\infty} \langle \psi_A | F_n | \psi_A \rangle \\
\text{where } F_n &= (-i)^n \int d^4 x_1 \dots d^4 x_n \Theta_{01\dots n} \mathcal{F}_n, \\
\text{and } \mathcal{F}_n &= [\mathcal{F}_{n-1}, \mathcal{H}_n] \quad \text{with } \mathcal{F}_0 \equiv B_0,
\end{aligned} \tag{2.7}$$

where $H_{\text{int}}(t) = \int d^3 \mathbf{x} \mathcal{H}(x)$. Each term in the n th order perturbation operator \mathcal{F}_n involves n spacetime points x_i , located progressively further back in time as i increases.

An expression for the commutator of functions of field operators with the Pauli-Jordan function defined by $[\phi_j, \phi_i] = \Delta_{ij}$ can be found in [2]. For our perturbation series,

$$\begin{aligned}
&[\mathcal{F}_{r-1}(\phi_0, \phi_1, \dots, \phi_{r-1}), \mathcal{H}(\phi_r)] \\
&= - \underbrace{\sum_{k_0=0}^{\infty} \sum_{k_1=0}^{\infty} \dots \sum_{k_{r-1}=0}^{\infty}}_{K_r \equiv \sum_{i=0}^{r-1} k_i \neq 0} \left(\prod_{i=0}^{r-1} \frac{(\Delta_{ir})^{k_i}}{k_i!} \right) D_0^{k_0} D_1^{k_1} \dots D_{r-1}^{k_{r-1}} \mathcal{F}_{r-1} D_r^{K_r} \mathcal{H} \\
&\equiv \mathcal{F}_r(\phi_0, \phi_1, \dots, \phi_r).
\end{aligned} \tag{2.8}$$

The operator D_i is defined via $D_i[\phi_0^{n_0} \phi_1^{n_1} \dots \phi_i^{n_i} \dots] = (\phi_0^{n_0} \phi_1^{n_1} \dots n_i \phi_i^{n_i-1} \dots)$ and the sums k_i run from zero to infinity, with the exclusion of the case in which all are simultaneously zero. Every one of the n iterations ($r=1, \dots, n$) required to generate \mathcal{F}_n from \mathcal{F}_0 generates a set of terms, each of which contains at least one factor of Δ_{ir} for some $i < r$. Each term in \mathcal{F}_n therefore refers to a set of spacetime points $x_0, x_1, \dots, x_i, \dots, x_r, \dots, x_n$ in which every member x_i is connected to at least one earlier point x_r by a retarded propagator. Thus every non-zero contribution to the sensitivity σ_B of the detector must contain an unbroken chain of retarded propagators from a point in the source.

Phi-cubed theory. As an illustrative example we shall suppose that $B(t_0) = \phi(t_0, \mathbf{x}_0) = \phi(x_0)$ and

$$\mathcal{H}(x) = \frac{g}{3!}\phi_x^3 - \gamma J_x \phi_x .$$

We assume that the system can be approximated by the vacuum of the non-interacting theory at $t = -\infty$, i.e. we take $|\psi_A\rangle = |0\rangle$.

The first-order commutator is

$$\begin{aligned} \mathcal{F}_1 &= [\phi_0, \mathcal{H}_1] = \frac{g}{3!}[\phi_0, \phi_1^3] - \gamma J_1[\phi_0, \phi_1] \\ &= -\left(\frac{g}{2}\phi_1^2 - \gamma J_1\right)\Delta_{01} , \end{aligned} \quad (2.9)$$

where $J_i \equiv J(x_i)$. This gives

$$F_1 = -i \int d^4x_1 \left(\frac{g}{2}\phi_1^2 - \gamma J_1\right) \Delta_{01}^R , \quad (2.10)$$

where $\Delta_{ij}^R \equiv \Delta_R(x_i, x_j) = -\Theta(x_i^0 - x_j^0)\Delta_{ij}$ is the retarded propagator for the free field.¹ Note the relative minus sign due to our definition of $\Delta_{ij} = [\phi_j, \phi_i]$.

The second-order commutator $\mathcal{F}_2 = [\mathcal{F}_1, \mathcal{H}_2]$ is then

$$\begin{aligned} \mathcal{F}_2 &= -\frac{g^2}{12}\Delta_{01}[\phi_1^2, \phi_2^3] + \gamma J_2 \frac{g}{2}\Delta_{01}[\phi_1^2, \phi_2] \\ &= \frac{g}{2} \left\{ g(\phi_1\phi_2^2 + \phi_2\Delta_{12}) - 2\gamma J_2\phi_1 \right\} \Delta_{12}\Delta_{01} . \end{aligned} \quad (2.11)$$

Finally, the third-order commutator is

$$\begin{aligned} \mathcal{F}_3 &= \frac{g}{2} \left\{ -g^2 \left(\phi_1\phi_2\phi_3^2 + \phi_1\phi_3\Delta_{23} + 2\phi_2\phi_3\Delta_{13} + \Delta_{23}\Delta_{13} + \frac{1}{2}\phi_3^2\Delta_{12} \right) \Delta_{23} \right. \\ &\quad - \frac{1}{2}g^2\phi_2^2\phi_3^2\Delta_{13} + g\gamma J_2\phi_3^2\Delta_{13} + g\gamma J_3 \left(2\phi_1\phi_2\Delta_{23} + \phi_2^2\Delta_{13} + \Delta_{23}\Delta_{12} \right) \\ &\quad \left. - 2\gamma^2 J_2 J_3 \Delta_{13} \right\} \Delta_{12}\Delta_{01} . \end{aligned} \quad (2.12)$$

We may now evaluate the expectation value of B . Any uncontracted field operators can be handled using Wick's Theorem and give rise to Feynman propagators:

$$\Delta_{ij}^F \equiv \Delta_F(x_i, x_j) = \langle 0 | T[\phi_i\phi_j] | 0 \rangle . \quad (2.13)$$

It then follows that the first term in the expectation value expansion eq. (2.7) is, from eq. (2.10),

$$\langle 0 | F_1 | 0 \rangle = -i \int d^4x_1 \left(\frac{g}{2}\Delta_{11}^F - \gamma J_1\right) \Delta_{01}^R . \quad (2.14)$$

¹The relevant propagators are defined in appendix B.

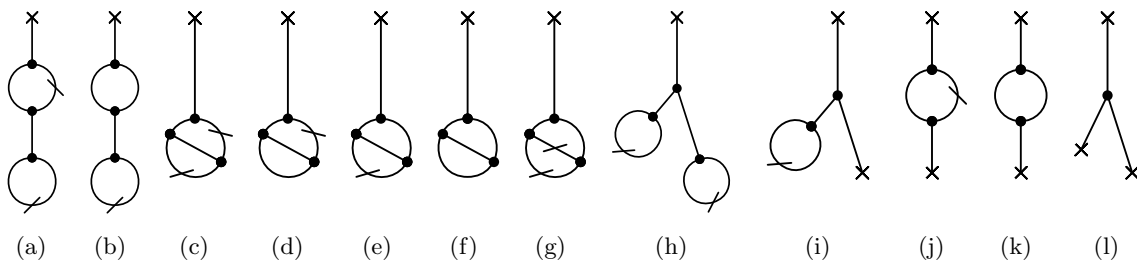


Figure 1. The diagrams corresponding to $\langle 0|F_3|0\rangle$. The co-ordinate x_0 is labelled by the cross at the top of each graph and the lower points are at x_1 , x_2 and x_3 . The time-ordering of x_2 and x_3 in diagrams (h), (i) and (l) is no longer fixed by retarded propagators. Retarded propagators are represented by unslashed lines and Feynman propagators by slashed lines.

The second term, from eq. (2.11), involves an odd number of fields and therefore vanishes. The third term, from eq. (2.12) and depicted in figure 1, is

$$\begin{aligned}
\langle 0|F_3|0\rangle = ig \int d^4x_1 d^4x_2 d^4x_3 \left\{ g^2 \left(\frac{1}{2} \Delta_{12}^F \Delta_{33}^F + \Delta_{13}^F \Delta_{23}^F - \frac{1}{2} \Delta_{13}^F \Delta_{23}^R - \Delta_{23}^F \Delta_{13}^R \right. \right. \\
+ \frac{1}{2} \Delta_{23}^R \Delta_{13}^R - \frac{1}{4} \Delta_{33}^F \Delta_{12}^R \Big) \Delta_{23}^R + g^2 \left(\frac{1}{8} \Delta_{22}^F \Delta_{33}^F + \frac{1}{4} (\Delta_{23}^F)^2 \right) \Delta_{13}^R \\
\left. \left. - g\gamma J_3 \left(\frac{1}{2} \Delta_{22}^F \Delta_{13}^R + \Delta_{12}^F \Delta_{23}^R - \frac{1}{2} \Delta_{23}^R \Delta_{12}^R \right) + \frac{1}{2} \gamma^2 J_2 J_3 \Delta_{13}^R \right\} \Delta_{12}^R \Delta_{01}^R \quad (2.15)
\end{aligned}$$

Of particular note is the $\Delta_{22}^F \Delta_{33}^F$ term on the second line (which corresponds to figure 1(h)). This includes an extra factor of 1/2 because there is a residual Heaviside function, Θ_{23} , that cannot be absorbed into the retarded propagators. However, because of the symmetry under interchange of $2 \leftrightarrow 3$ we can drop the time-ordering constraint in exchange for a symmetry factor of 1/2!. The same Heaviside function is also present in the term $\propto J_2 J_3$ (see figure 1(l)) and its elimination also gives rise to a factor 1/2. For these two diagrams, we say that points 2 and 3 are ‘equivalent’. Finally, the $\Delta_{22}^F \Delta_{13}^R J_3$ term on the final line (see figure 1(i)) also originally had a Θ_{23} which we eliminated by combining it with a contribution $\propto \Delta_{33}^F \Delta_{12}^R J_2$. In this way all explicit time-ordering Heaviside functions disappear from the final expression.

From the first few nested commutators, it is evident that the majority of the terms in $\langle 0|B|0\rangle$ are vacuum diagrams, which contribute nothing to the sensitivity of the detector to the source.

It is also apparent that there is a straightforward relationship between the set of diagrams that can be drawn and the form of a given nested commutator. The rules are listed below for the case $B(t_0) = \phi(t_0)$.

Feynman rules. To compute \mathcal{F}_n we are to draw a set of skeleton graphs involving the $n + 1$ times from t_0 to t_n . The graphs can be built up iteratively starting from the latest time, t_0 , and ending with the earliest time t_n . We are to draw either a cubic interaction vertex (arising from $g\phi^3/3!$) or a source term (arising from $\gamma J_n \phi$) for all times t_1 to t_n inclusive. For each time earlier than t_0 there must be at least one retarded propagator

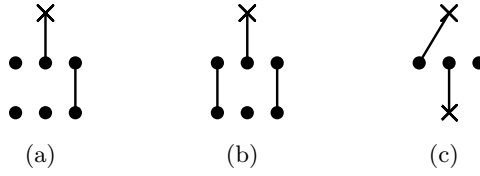


Figure 2. The three contributions to \mathcal{F}_2 . A horizontal row of dots represents a vertex and any uncontracted dots are understood as field operators. The graphs have an associated combinatoric and coupling factor: for (a) and (b) this is $18(g/3!)^2$ and for (c) it is $6(g/3!)(-\gamma J_2)$.

heading forwards in time. This means that the vertices may include uncontracted field operators (i.e. there can be fewer than 3 retarded propagators at any vertex but never zero). For each vertex we associate a factor of $g/3!$ and a factor of ϕ_i for each uncontracted field operator (written in chronological order). For each instance of the source there is a factor of $-\gamma J_i$ and there is an overall factor of $(-1)^n$. For each retarded propagator between x_j (earlier) and x_i (later) associate a factor of Δ_{ij} . There is a combinatoric factor for the number of different ways to contract the fields in forming the retarded propagators. This is the prescription to compute the operator \mathcal{F}_n and it is illustrated for the case of \mathcal{F}_2 in figure 2.

To compute $\langle 0|F_n|0\rangle$ we take each skeleton, convert the Δ_{ij} to $-\Delta_{ij}^R$ and compute the vacuum Green’s functions associated with the incomplete vertices using Wick’s Theorem. There is a factor $-i \int d^4x_i$ for all $i > 0$ and we must take care to absorb the time-ordering Heaviside functions into the retarded propagators: if any Heaviside functions remain then they can be eliminated provided we associate a symmetry factor of $1/m!$ if there are m ‘equivalent’ spacetime points (in the sense explained above). For example, there is a factor $1/2$ for graphs (h) and (l) in figure 1.

3 Scattering amplitudes

We use the following expression for the scattering amplitude in the presence of a detector source K_x and a production source J_x :

$$\Gamma_{JK} = \langle T| \left[\text{T exp} \left(i \int_T^\infty d^4x K_x \phi_x \right) \right] |T\rangle \quad (3.1)$$

where $|T\rangle \equiv U(T, -\infty)|0\rangle$ and

$$U(t', t) \equiv \text{T exp} \left(-i \int_t^{t'} d^4x (H_{\text{int}}(x) - J_x \phi_x) \right). \quad (3.2)$$

Again we take

$$H_{\text{int}}(x) = \frac{g}{3!} \phi_x^3. \quad (3.3)$$

We will assume that K_x has support only in the future of T and that the cubic interaction and source J_x are turned off in that region. The situation is illustrated in figure 3. Equation (3.1) looks just like an “in-in” expectation value and as such it inherits many of the

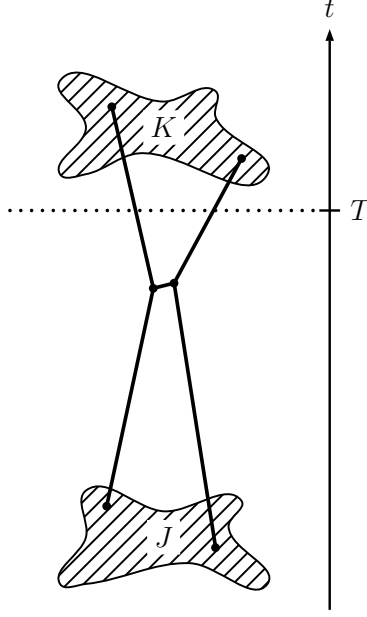


Figure 3. Source-to-detector scattering.

properties described in the previous section. Eq. (3.1) is a scattering amplitude in the sense that $\exp(i \int_T^\infty d^4x K_x \phi_x)$ is rather like an S-matrix operator for determining the future of the state $|T\rangle$. For simplicity, we have assumed that the detector acts locally, e.g. there are no bilocal terms $\sim K(x, y)\phi(x)\phi(y)$.

In the case of n -to-two scattering, we can extract the relevant part of the amplitude, $\Gamma_{JK}^{n \rightarrow 2}$, from

$$\sum_{n=0}^{\infty} \Gamma_{JK}^{n \rightarrow 2} = - \int d^4x d^4y \frac{1}{2} K_x K_y \langle 0 | U^\dagger(T, -\infty) \mathbb{T}[\phi_x \phi_y] U(T, -\infty) | 0 \rangle. \quad (3.4)$$

As in the previous section, and since we are assuming $x^0, y^0 > T$, eq. (3.4) can be re-arranged by commuting $\phi_x \phi_y$ through the time-evolution operator using the Baker-Hausdorff lemma, i.e.

$$U^\dagger(T, -\infty) \phi_x \phi_y U(T, -\infty) = \sum_n F_n \quad (3.5)$$

where

$$F_n = (-i)^n \prod_{j=1}^n \int d^4x_j \Theta_{T1\dots n} \mathcal{F}_n \quad (3.6)$$

and

$$\mathcal{F}_n = [\mathcal{F}_{n-1}, \mathcal{H}_n] \quad \text{with} \quad \mathcal{F}_0 = \phi_x \phi_y \quad \text{and} \quad \mathcal{H}_n = g \phi_n^3 / 3! - J_n \phi_n. \quad (3.7)$$

To compute two-to-two scattering at tree-level we would need to compute the part of \mathcal{F}_4 that is proportional to $J^2 g^2$.

The amplitude can also be obtained using the same Feynman rules as articulated in the previous section. The only difference is that the field operator that we are averaging

can be a non-local polynomial of the field. This merely introduces extra points, all later than the time T , at which propagators may terminate. For each such point we will have a factor of $-i \int d^4x_i K_i$.

Some examples at tree-level. We begin by considering the one-to-two amplitude, which is

$$\begin{aligned} \Gamma_{JK}^{1 \rightarrow 2} &= -g \prod_{j=1}^2 \left(\int d^4x_j \right) \int d^4x \int d^4y \Theta_{xT} \Theta_{yT} \Theta_{T1} \\ &\quad \times \frac{1}{2} K_x K_y J_2 \left[\Delta_{x1}^R \left(\Delta_{y1}^F - \frac{1}{2} \Delta_{y1}^R \right) \Delta_{12}^R + (x \leftrightarrow y) \right]. \end{aligned} \quad (3.8)$$

Notice that this includes a Feynman propagator coupling from the interaction vertex to the detector. There is however no violation of causality because the measurement is the coherent detection of two particles at points x and y , which is causal since one of those particles is constrained to lie in the future lightcone of the source by the unbroken chain of retarded propagators. In fact we should anticipate such superficially acausal correlations: they are a manifestation of entanglement.

We will now consider two-to-two scattering. In this case, the Feynman rules give

$$\begin{aligned} \Gamma_{JK}^{2 \rightarrow 2} &= -g^2 \prod_{j=1}^4 \left(\int d^4x_j \right) \int d^4x \int d^4y \Theta_{xT} \Theta_{yT} \Theta_{T1} \frac{1}{2} K_x K_y J_3 J_4 \\ &\quad + \left\{ [\Delta_{x1}^R \left(\Delta_{y1}^F - \frac{1}{2} \Delta_{y1}^R \right) \Delta_{12}^R \Delta_{23}^R \Delta_{24}^R + (x \leftrightarrow y)] \right. \\ &\quad \quad \quad \left. + \{ [\Delta_{x1}^R \Delta_{13}^R \Delta_{y2}^R \Delta_{24}^R (\Delta_{12}^F \Theta_{12} - \Delta_{12}^R) + (1 \leftrightarrow 2)] + [3 \leftrightarrow 4] \} \right. \\ &\quad \quad \quad \left. + \{ [\Delta_{x1}^R \Delta_{13}^R \Delta_{y2}^F \Delta_{24}^R + (1 \leftrightarrow 2)] \Delta_{12}^R + [3 \leftrightarrow 4] \} \right\}. \end{aligned} \quad (3.9)$$

The first line in the large braces of eq. (3.9) is the s -channel contribution, and the first set of terms in brackets on each of the third and fourth lines generates the t -channel contribution. The u -channel contribution is obtained from the $[3 \leftrightarrow 4]$ interchange of the t -channel contribution. Note the residual Θ_{12} on the second line. It combines with a Θ_{21} term after interchange $(1 \leftrightarrow 2)$. Equation (3.9) can be simplified somewhat by symmetrizing the sources:

$$\begin{aligned} \Gamma_{JK}^{2 \rightarrow 2} &= -g^2 \prod_{j=1}^4 \left(\int d^4x_j \right) \int d^4x \int d^4y \Theta_{xT} \Theta_{yT} \Theta_{T1} K_x K_y J_3 J_4 \\ &\quad \times \left\{ \frac{1}{4} \Delta_{x1}^R (2\Delta_{y1}^F - \Delta_{y1}^R) \Delta_{12}^R \Delta_{23}^R \Delta_{24}^R \right. \\ &\quad \quad \quad \left. + \frac{1}{2} \Delta_{x1}^R \Delta_{13}^R \Delta_{y2}^R \Delta_{24}^R (\Delta_{12}^F - 2\Delta_{12}^R) + \Delta_{x1}^R \Delta_{13}^R \Delta_{y2}^F \Delta_{24}^R \Delta_{12}^R \right\}. \end{aligned} \quad (3.10)$$

Written in this form, there are only 5 distinct graphs to consider and these are illustrated in figure 4.

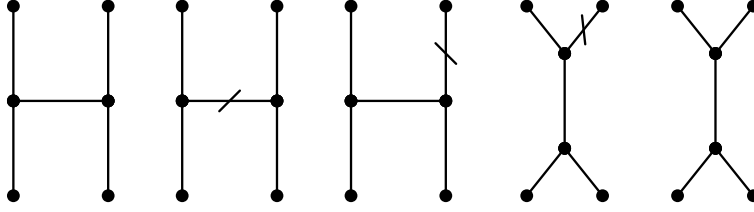


Figure 4. The five graphs relevant for 2-to-2 scattering. Retarded propagators are represented by unslashed lines and Feynman propagators by slashed lines.

We can make explicit contact with the corresponding S-matrix amplitude for the scattering of momentum eigenstates by promoting the sources K and J to operators in Fock space. Specifically, if we take K and J to be replaced by

$$\begin{aligned} K_x &\rightarrow \phi_x^{\text{out}}(\square_x^2 + m^2), \\ J_x &\rightarrow \phi_x^{\text{in}}(\square_x^2 + m^2), \end{aligned} \quad (3.11)$$

and we take the limit $T \rightarrow \infty$ in such a way that the integrals over x^0 and y^0 can be approximated by integration over an infinite time domain, which allows the preparation of freely-propagating momentum eigenstates at $t \rightarrow \pm \infty$. We may then take the overlap of eq. (3.10) with two-particle “in” and “out” states, i.e.

$$\mathcal{M}_{JK}^{2 \rightarrow 2} \equiv \langle \text{out}; \mathbf{k}_3, \mathbf{k}_4 | \Gamma_{JK}^{2 \rightarrow 2} | \text{in}; \mathbf{k}_1, \mathbf{k}_2 \rangle. \quad (3.12)$$

After expressing the 5 propagators in eq. (3.10) in momentum space, the spacetime integrals can be performed leaving behind an overall energy-momentum conserving delta function. The final result is as expected:

$$\mathcal{M}_{JK}^{2 \rightarrow 2} = -g^2 (2\pi)^4 \delta^{(4)}(k_1 + k_2 - k_3 - k_4) \left(\frac{i}{s - m^2} + \frac{i}{t - m^2} + \frac{i}{u - m^2} \right), \quad (3.13)$$

where $s = (k_1 + k_2)^2$, $t = (k_1 - k_2)^2$ and $u = (k_1 - k_3)^2$ are the Mandelstam variables. To illustrate the point, the last two graphs of figure 4, which correspond to the first two terms in the second line of eq. (3.10), contribute to the s -channel amplitude with weights $2 - 1 = 1$.

The correspondence also works out for $2 \rightarrow 3$ at tree-level. In this case, there are three topologies to consider, as illustrated in figure 5(a). Figure 5(b) shows the graphs corresponding to the first topology in figure 5(a). Each graph should be summed over all allowed time orderings (i.e. subject to the rule that there must always be at least one retarded propagator heading forwards from any vertex) and agreement with the S-matrix calculation follows, e.g. for the graphs in figure 5(b) the relative weights are (in order from the first to the last graph) $3 - 1 - 1 - 1 - 6 + 2 + 2 + 2 + 1 = 1$ and we have doubled the contribution from graphs 5 - 8 to account for the contribution where the Feynman and retarded propagators are swapped on the rightmost pair of outgoing legs. The two other types of graph shown in figure 5(a) also each have a total weight equal to 1. An all orders proof of the equivalence with the S-matrix, in the case of positive energy plane-wave scattering, is provided in section 5.

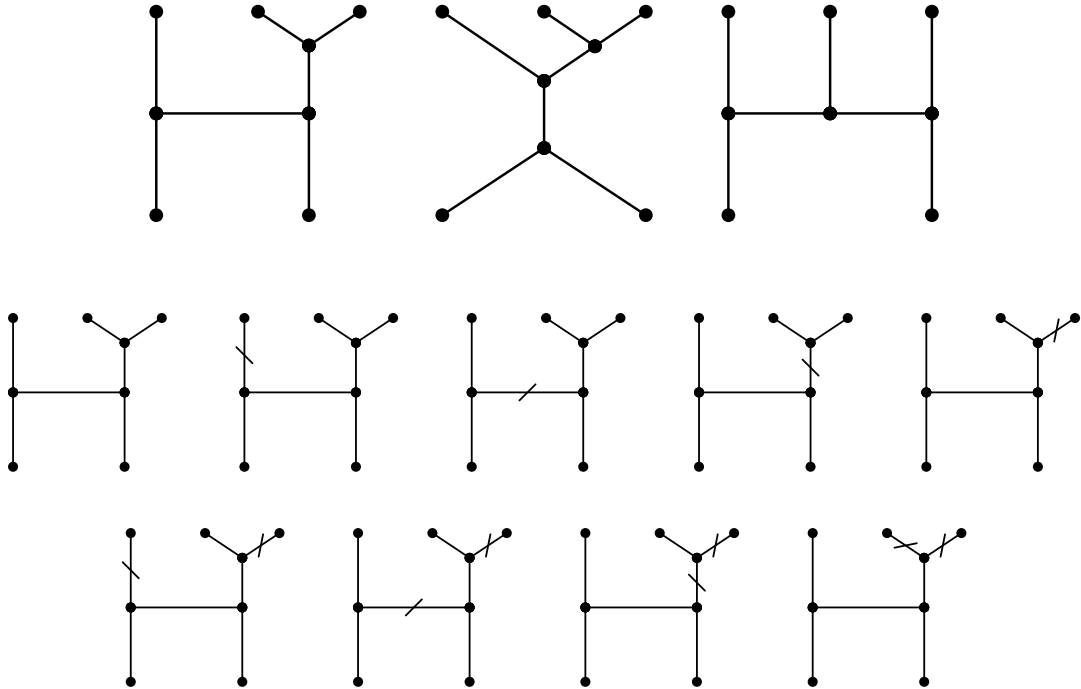


Figure 5. (a) The topologies relevant to 2-to-3 scattering; (b) The graphs corresponding to the first topology in (a).

4 Path integral representation

In this section we will explain the connection of the operator-level amplitudes in the previous section to the retarded amplitudes of thermal field theory. To this end, we will apply the “in-in” or closed-time path (CTP) formalism due to Schwinger and Keldysh [3, 4]. In real-time formulations of quantum field theory at finite temperature and density (see e.g. [5] and references therein), it is known that physical reaction rates must be calculated from the absorptive parts of *retarded* self-energies in order to obtain the correct quantum statistics [6, 7]. We emphasise that retarded self-energies have arisen naturally in our treatment thus far (e.g. see the diagrams in figure 1).

The starting point of the “in-in” generating functional is the partition function:

$$Z = \text{tr } \rho \tag{4.1}$$

where the density operator ρ represents the detection subsystem, which we suppose to act in the time interval $[T_1, T_2]$. Contained in this generating functional is the amplitude Γ_{JK} from the previous section, since, in the Heisenberg picture, we can write $\Gamma_{JK} = \langle 0|\rho|0\rangle$ where

$$\rho = \text{T exp} \left(i \int_T^\infty d^4x K_x \phi_x^H \right) . \tag{4.2}$$

To build the path integral, we prepare a set of N independent detectors, each described by a density operator ρ_i and whose actions have exclusive support over infinitesimal intervals $\Delta t = t_{i+1} - t_i = (T_1 - T_2)/N$, where $t_i \in [T_1, T_2]$. In the continuous limit,

$N \rightarrow \infty$, the density operator of the combined system of detectors may be written as the product integral

$$\rho = \prod_{T_1}^{T_2} \rho(t)^{dt}. \quad (4.3)$$

In order to generate a path-integral representation of the partition function Z , we imagine perturbing the evolution of the system by means of some unphysical test source j_x . Thus, we insert into eq. (4.1) unity in the form

$$\overline{\text{T}} \exp \left[-i \int_{T_A}^{T_B} d^4x j_x \phi_x^{\text{H}} \right] \text{T} \exp \left[i \int_{T_A}^{T_B} d^4x j_x \phi_x^{\text{H}} \right] = \mathbb{I}. \quad (4.4)$$

Notice that this insertion will generate two paths of evolution: \mathcal{C}_+ , running forwards in time from T_A to T_B and \mathcal{C}_- , running backwards from T_B and T_A . It is the presence of these two anti-parallel integration contours that gives rise to the closed-time path $\mathcal{C} = \mathcal{C}_+ \cup \mathcal{C}_-$ of the ‘‘in-in’’ formalism. Hereafter, objects with time arguments confined to the positive (time-ordered) branch are denoted by a subscript ‘+’ and those with time arguments confined to the negative (anti-time-ordered) branch are denoted by a subscript ‘-’. We note that the time T_A is the boundary time of the evolution of the system at which the initial conditions are specified.² Ultimately, we will take the limits $T_A \rightarrow -\infty$ assuming that, asymptotically, the system is the free vacuum.

By further inserting complete sets of eigenstates of the Heisenberg-picture field operator ϕ_x^{H} , we may develop the path-integral representation of the generating functional:

$$Z[j^a] = \int [d\phi_{\mathbf{z}}^a] \langle \phi_{\mathbf{z}}^-, T_B | \rho | \phi_{\mathbf{z}}^+, T_B \rangle \exp \left[i \left(S[\phi^a; T_A, T_B] + i \int_{T_A}^{T_B} d^4x \eta_{ab} j_x^a \phi_x^b \right) \right], \quad (4.5)$$

where $[d\phi_{\mathbf{z}}^a] = \prod_{T_A}^{T_B} [d\phi_t^a(\mathbf{z})]^{dt}$ denotes functional integration over ‘+’ and ‘-’ field configurations. The test sources and fields have been written in the doublet notation employed in [8–10], where

$$j_x^a = \left(j_x^+, j_x^- \right), \quad j_{a,x} = \eta_{ab} j_x^b = \left(j_x^+, -j_x^- \right) \quad (4.6a)$$

$$\phi_x^a = \left(\phi_x^+, \phi_x^- \right), \quad \phi_{a,x} = \eta_{ab} \phi_x^b = \left(\phi_x^+, -\phi_x^- \right) \quad (4.6b)$$

and $\eta_{ab} = \text{diag}(1, -1)$. Hereafter, CTP indices, labelling the confinement of objects to the positive and negative branches of the CTP contour, are denoted by the lower-case Roman characters $a, b = 1, 2 \equiv +, -$. In the same notation, the action $S[\phi^a; T_A, T_B]$ may be written

$$S[\phi^a; T_A, T_B] = \int_{T_A}^{T_B} d^4x \left[\frac{1}{2} \eta_{ab} \left(\partial_\mu \phi_x^a \partial^\mu \phi_x^b - m^2 \phi_x^a \phi_x^b \right) + \mathcal{L}^{\text{int}}(\phi^a) \right], \quad (4.7)$$

where the interaction part is

$$\mathcal{L}^{\text{int}}(\phi^a) = \eta_{ab} J_x^a \phi_x^b - \frac{g}{3!} \eta_{abc} \phi_x^a \phi_x^b \phi_x^c. \quad (4.8)$$

²For a discussion of the importance of keeping track of this boundary time in non-equilibrium phenomena see [5].

It contains the physical emission sources

$$J^a = (J_x, J_x) . \quad (4.9)$$

The tensor η_{abc} , appearing in eq. (4.8), is defined such that

$$\eta_{abc} = \begin{cases} +1 , & a = b = c = 1 \\ -1 , & a = b = c = 2 \\ 0 , & \text{otherwise.} \end{cases} \quad (4.10)$$

We may introduce an operator $\sqrt{\rho}$ and write the kernel of the density operator in the form

$$\langle \phi_{\mathbf{z}}^-, T_B | \rho | \phi_{\mathbf{z}}^+, T_B \rangle = \langle \phi_{\mathbf{z}}^-, T_B | (\sqrt{\rho})^2 | \phi_{\mathbf{z}}^+, T_B \rangle . \quad (4.11)$$

Again, by inserting complete sets of eigenstates of the Heisenberg field operator, we obtain

$$\begin{aligned} \langle \phi_{\mathbf{z}}^-, T_B | \rho | \phi_{\mathbf{z}}^+, T_B \rangle &\sim \int [d\phi_{T_2}^a(\mathbf{z})] \langle \phi_{\mathbf{z}}^-, T_1 | \sqrt{\rho} | \phi_{\mathbf{z}}^-, T_2 \rangle \langle \phi_{\mathbf{z}}^+, T_2 | \sqrt{\rho} | \phi_{\mathbf{z}}^+, T_1 \rangle \\ &\sim \int [d\phi_{\mathbf{z}}^a] \exp\left(iK[\phi^a; T_1, T_2]\right) , \end{aligned} \quad (4.12)$$

where $[d\phi_{\mathbf{z}}^a] = \prod_{T_1}^{T_2} [d\phi_t^a(\mathbf{z})]^{dt}$ and to simplify matters we henceforth assume $T_1 = T_B = T$ (this definition of T matches that in the previous section).

In general, the exponent $K[\phi^a; T_1, T_2]$ will be expressed as an infinite series of convolutions of poly-local sources and fields of the form $K_{abc\dots xyz\dots} \phi_x^a \phi_y^b \phi_z^c \dots$. However, for our purposes, we shall take $K[\phi^a; T_1, T_2]$ to contain only a local source, i.e.

$$K[\phi^a; T_1, T_2] = \frac{1}{2} \int_{T_1}^{T_2} d^4x K_{a,x} \phi_x^a , \quad (4.13)$$

where

$$K_x^a = (K_x, -K_x) . \quad (4.14)$$

Notice that K_x^a differs by a sign in the second element relative to the emission source J_x^a . This relative sign and the overall factor of $1/2$ in eq. (4.13) arise from writing $\rho = (\sqrt{\rho})^2$.

Thus, we arrive at the form of the ‘‘in-in’’ generating functional for our choice of density operator:

$$Z[j^a] = \int [d\phi_{\mathbf{z}}^a] \exp\left[\frac{i}{2} \int_{T_1}^{T_2} d^4x \eta_{ab} K_x^a \phi_x^b\right] \exp\left[i\left(S[\phi^a; T_A, T_B] + \int_{T_A}^{T_B} d^4x \eta_{ab} j_x^a \phi_x^b\right)\right] . \quad (4.15)$$

Completing the square in the free part of the action, we write

$$\phi_x'^a = \phi_x^a - i \int_{T_A}^{T_B} d^4y \Delta_{xy}^{ab} j_{b,y} , \quad (4.16)$$

where

$$\Delta_{xy}^{ab} = \begin{bmatrix} \Delta_{xy}^F & \Delta_{xy}^< \\ \Delta_{xy}^> & \Delta_{xy}^D \end{bmatrix} \quad (4.17)$$

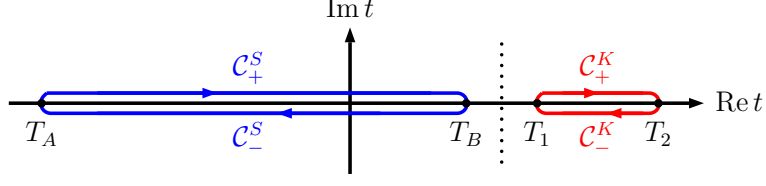


Figure 6. The two closed contours corresponding to the time integrals in eq. (4.18).

is the free 2×2 CTP matrix propagator. With this shift in the field, we may recast the “in-in” generating functional in the form

$$Z[j^a] = Z_0[0] \exp \left[\frac{1}{2} \int_{T_1}^{T_2} d^4x K_{a,x} \delta_x^a \right] \exp \left[i \int_{T_A}^{T_B} d^4x \mathcal{L}^{\text{int}}(-i\delta_x^a) \right] \times \exp \left[-\frac{1}{2} \iint_{-\infty}^{+\infty} d^4x d^4y j_{a,x} \Delta_{xy}^{ab} j_{b,y} \right] \quad (4.18)$$

where $Z_0[0]$ is the generating functional in the absence of interactions and for vanishing test sources $j_{a,x}$ and we have introduced the short-hand notation

$$\delta_x^a \equiv \frac{\delta}{\delta j_{a,x}} \quad (4.19)$$

for functional derivatives with respect to the test sources. The two time integrals over the intervals $[T_A, T_B]$ and $[T_1, T_2]$ have given rise to two closed-time paths, as illustrated in figure 6, each corresponding to one of the subsystems into which the system has been partitioned. We will take $T_A \rightarrow -\infty$, $T_B = T_1 = T$ and $T_2 \rightarrow +\infty$.

By means of an orthogonal transformation, we may rotate to the Keldysh basis (e.g. see [5, 11]):

$$\tilde{\Delta}_{xy}^{ab} = O^a_c O^b_d \Delta_{xy}^{cd} = \begin{bmatrix} 0 & \Delta_{xy}^A \\ \Delta_{xy}^R & \Delta_{xy}^1 \end{bmatrix}, \quad O^{ab} = \frac{1}{\sqrt{2}} \begin{bmatrix} 1 & 1 \\ 1 & -1 \end{bmatrix} \quad (4.20)$$

in which the elements of the CTP propagator comprise the retarded, advanced and Hadamard propagators (see appendix B). With this transformation

$$Z[\tilde{j}^a] = Z_0[0] \exp \left[\frac{1}{\sqrt{2}} \int_{T_1}^{T_2} d^4x K_x \frac{\delta}{\delta \tilde{j}_{-,x}^a} \right] \exp \left[i \int_{T_A}^{T_B} d^4x \mathcal{L}^{\text{int}} \left(\frac{1}{i} \frac{\delta}{\delta \tilde{j}_{a,x}^a} \right) \right] \times \exp \left[-\frac{1}{2} \iint_{-\infty}^{+\infty} d^4x d^4y \tilde{j}_{a,x} \tilde{\Delta}_{xy}^{ab} \tilde{j}_{b,y} \right], \quad (4.21)$$

where we have defined

$$\tilde{j}_x^a = (\tilde{j}_x^+, \tilde{j}_x^-) \quad (4.22)$$

with

$$\tilde{j}_x^\pm = \frac{1}{\sqrt{2}} (j_x^+ \pm j_x^-). \quad (4.23)$$

Subsequently, contracting the CTP indices in the exponents of eq. (4.21), we obtain

$$Z[\tilde{j}^a] = Z_0[0] \exp \left[\frac{1}{\sqrt{2}} \int_{T_1}^{T_2} d^4x K_x \tilde{\delta}_x^- \right] \exp \left[i \int_{T_A}^{T_B} d^4x \mathcal{L}^{\text{int}}(-i\delta_x^a) \right] \\ \times \exp \left[-\frac{1}{2} \iint_{-\infty}^{+\infty} d^4x d^4y \left(\tilde{j}_x^- \Delta_{xy}^R \tilde{j}_y^+ + \tilde{j}_x^+ \Delta_{xy}^A \tilde{j}_y^- + \tilde{j}_x^- \Delta_{xy}^1 \tilde{j}_y^- \right) \right] \quad (4.24)$$

in which

$$\mathcal{L}^{\text{int}}(-i\delta_x^a) = -i \left[\sqrt{2} J_x \tilde{\delta}_x^+ + \frac{g}{3! \sqrt{2}} \left((\tilde{\delta}_x^+)^3 + 3 \tilde{\delta}_x^+ (\tilde{\delta}_x^-)^2 \right) \right] \quad (4.25)$$

and we have used the fact that

$$\delta_x^\pm = \frac{1}{\sqrt{2}} (\tilde{\delta}_x^+ \pm \tilde{\delta}_x^-). \quad (4.26)$$

After suitable changes of variables and using the relations

$$\Delta_{xy}^R = \Delta_{yx}^A, \quad \Delta_{xy}^1 = 2\Delta_{xy}^F - \Delta_{xy}^R - \Delta_{xy}^A, \quad (4.27)$$

the Keldysh representation of the “in-in” generating functional eq. (4.24) may re-expressed as

$$Z[\tilde{j}^a] = Z_0[0] \exp \left[\frac{1}{\sqrt{2}} \int_x K_x \tilde{\delta}_x^- \right] \exp \left[\sqrt{2} \int_x J_x \tilde{\delta}_x^+ \right] \exp \left\{ \frac{1}{3! \sqrt{2}} \int_x \left[(\tilde{\delta}_x^+)^3 + 3(\tilde{\delta}_x^-)^2 \tilde{\delta}_x^+ \right] \right\} \\ \times \exp \left\{ - \int_{xy} \left[\tilde{j}_x^- \Delta_{xy}^R \tilde{j}_y^+ + \tilde{j}_x^- (\Delta_{xy}^F - \Delta_{xy}^R) \tilde{j}_y^- \right] \right\}. \quad (4.28)$$

Equation (4.28) is the main result of this section. Notice in particular that *the physical source J couples only to the retarded propagator*.

An example. By way of illustration, we now consider the specific case of the one-to-two amplitude, obtained by expanding the exponentials in eq. (4.28) to second order in the detection sources K and to first order in the emission sources J :

$$\Gamma_{JK}^{1 \rightarrow 2} = \frac{g}{8} \int_{xyzw} K_x K_y J_w \tilde{\delta}_x^- \tilde{\delta}_y^- (\tilde{\delta}_z^-)^2 \tilde{\delta}_z^+ \tilde{\delta}_w^+ \\ \times \exp \left\{ - \int_{x'y'} \left[\tilde{j}_{x'}^- \Delta_{x'y'}^R \tilde{j}_{y'}^+ + \tilde{j}_{x'}^- (\Delta_{x'y'}^F - \Delta_{x'y'}^R) \tilde{j}_{y'}^- \right] \right\} \Big|_{\tilde{j}^a=0}. \quad (4.29)$$

Note that this amplitude is obtained directly from $Z[\tilde{j}^a]$. Acting with the rightmost functional derivative, we have

$$\Gamma_{JK}^{1 \rightarrow 2} = -\frac{g}{8} \int_{xyzw1} K_x K_y J_w \tilde{\delta}_x^- \tilde{\delta}_y^- (\tilde{\delta}_z^-)^2 \tilde{\delta}_z^+ \tilde{j}_1^- \Delta_{1w}^R \\ \times \exp \left\{ - \int_{x'y'} \left[\tilde{j}_{x'}^- \Delta_{x'y'}^R \tilde{j}_{y'}^+ + \tilde{j}_{x'}^- (\Delta_{x'y'}^F - \Delta_{x'y'}^R) \tilde{j}_{y'}^- \right] \right\} \Big|_{\tilde{j}^a=0}. \quad (4.30)$$

Performing the remaining \tilde{j}^+ functional derivative, we may neglect the first term in the exponent, giving

$$\Gamma_{JK}^{1 \rightarrow 2} = \frac{g}{8} \int_{xyzw12} K_x K_y J_w \tilde{\delta}_x^- \tilde{\delta}_y^- (\tilde{\delta}_z^-)^2 \times \tilde{j}_1^- \tilde{j}_2^- \Delta_{2z}^R \Delta_{1w}^R \exp \left\{ - \int_{x'y'} \tilde{j}_{x'}^- (\Delta_{x'y'}^F - \Delta_{x'y'}^R) \tilde{j}_{y'}^- \right\} \Big|_{\tilde{j}^- = 0}. \quad (4.31)$$

Differentiating again and using the fact that $\Delta_{xx}^R = 0$, we obtain

$$\Gamma_{JK}^{1 \rightarrow 2} = \frac{g}{8} \int_{xyzw2} K_x K_y J_w \tilde{\delta}_x^- \tilde{\delta}_y^- \tilde{\delta}_z^- j_2^- \Delta_{2z}^R \left[\Delta_{zw}^R - \int_{13} \tilde{j}_1^- \tilde{j}_3^- \Delta_{1w}^R (2\Delta_{3z}^F - \Delta_{3z}^R - \Delta_{3z}^A) \right] \times \exp \left\{ - \int_{x'y'} \tilde{j}_{x'}^- (\Delta_{x'y'}^F - \Delta_{x'y'}^R) \tilde{j}_{y'}^- \right\} \Big|_{\tilde{j}^- = 0}. \quad (4.32)$$

Finally, keeping only the connected diagrams, we have

$$\Gamma_{JK}^{1 \rightarrow 2} = -\frac{g}{4} \int_{xyzw12} K_x K_y J_w \tilde{\delta}_x^- \tilde{\delta}_y^- \tilde{j}_1^- \tilde{j}_2^- \Delta_{1z}^R (2\Delta_{2z}^F - \Delta_{2z}^R - \Delta_{2z}^A) \Delta_{zw}^R, \quad (4.33)$$

where integration variables have been relabelled for notational convenience. Performing the remaining functional derivatives, we arrive at the result

$$\Gamma_{JK}^{1 \rightarrow 2} = -\frac{g}{2} \int_{xyzw} K_x K_y \Delta_{xz}^R (2\Delta_{yz}^F - \Delta_{yz}^R - \Delta_{yz}^A) \Delta_{zw}^R J_w, \quad (4.34)$$

which is in agreement with eq. (3.8) since $x^0, y^0 > T$ and $z^0 < T$, so the advanced contribution vanishes.

5 Relation to S-matrix

In this section, we will show that the amplitudes calculated in the preceding sections are equivalent to the corresponding S-matrix amplitudes for the scattering of positive energy plane-waves. We begin by considering a general set of tree-level graphs with N_K outgoing external legs and N_J incoming external legs. The number of vertices V and propagators P are given by

$$V = N - 2, \quad P = 2N - 3 \quad (5.1)$$

in which $N = N_K + N_J$ is the total number of external legs. Expanding each of the exponentials in eq. (4.28) to the appropriate order, we have

$$\Gamma_{JK}^{N_J \rightarrow N_K} = (-1)^P \left(\frac{g}{\sqrt{2}} \right)^V \frac{1}{V^+!} \left(\frac{1}{3!} \int_x (\tilde{\delta}_x^+)^3 \right)^{V^+} \frac{1}{V^-!} \left(\frac{1}{2!} \int_x (\tilde{\delta}_x^-)^2 \tilde{\delta}_x^+ \right)^{V^-} \times \frac{1}{N_K!} \left(\frac{1}{\sqrt{2}} \int_x K_x \tilde{\delta}_x^- \right)^{N_K} \frac{1}{N_J!} \left(\sqrt{2} \int_x J_x \tilde{\delta}_x^+ \right)^{N_J} \times \frac{1}{P^+!} \left(\int_{xy} \tilde{j}_x^- \Delta_{xy}^R \tilde{j}_y^+ \right)^{P^+} \frac{1}{P^-!} \left(\frac{1}{2} \int_{xy} \tilde{j}_x^- (2\Delta_{xy}^F - \Delta_{xy}^R - \Delta_{xy}^A) \tilde{j}_y^- \right)^{P^-}, \quad (5.2)$$

where $V = V^+ + V^-$ and $P = P^+ + P^-$. For convenience of notation, we have left implicit the fact that the \tilde{j} are set to zero externally.

Using eq. (5.1), the factors of $\sqrt{2}$ in eq. (5.2) can be combined to give

$$\begin{aligned} \Gamma_{JK}^{N_J \rightarrow N_K} &= (-1)^P 2^{1-N_K} g^V \frac{1}{V^+!} \left(\frac{1}{3!} \int_x (\tilde{\delta}_x^+)^3 \right)^{V^+} \frac{1}{V^-!} \left(\frac{1}{2!} \int_x (\tilde{\delta}_x^-)^2 \tilde{\delta}_x^+ \right)^{V^-} \\ &\quad \times \frac{1}{N_K!} \left(\int_x K_x \tilde{\delta}_x^- \right)^{N_K} \frac{1}{N_J!} \left(\int_x J_x \tilde{\delta}_x^+ \right)^{N_J} \\ &\quad \times \frac{1}{P^+!} \left(\int_{xy} \tilde{j}_x^- \Delta_{xy}^R \tilde{j}_y^+ \right)^{P^+} \frac{1}{P^-!} \left(\frac{1}{2} \int_{xy} \tilde{j}_x^- (2\Delta_{xy}^F - \Delta_{xy}^R - \Delta_{xy}^A) \tilde{j}_y^- \right)^{P^-}. \end{aligned} \quad (5.3)$$

Performing the functional derivatives in the sources, we obtain

$$\begin{aligned} \Gamma_{JK}^{N_J \rightarrow N_K} &= (-1)^P 2^{1-N_K} g^V \frac{1}{V^+!} \left(\frac{1}{3!} \int_x (\tilde{\delta}_x^+)^3 \right)^{V^+} \frac{1}{V^-!} \left(\frac{1}{2!} \int_x (\tilde{\delta}_x^-)^2 \tilde{\delta}_x^+ \right)^{V^-} \\ &\quad \times \frac{1}{N_K!} \left(\int_{xy} K_x \Delta_{xy}^R \tilde{j}_y^+ \right)^{N_K^+} \left(\int_{xy} K_x (2\Delta_{xy}^F - \Delta_{xy}^R) \tilde{j}_y^- \right)^{N_K^-} \\ &\quad \times \frac{1}{N_J!} \left(\int_{xy} \tilde{j}_x^- \Delta_{xy}^R J_y \right)^{N_J} \frac{1}{(P^+ - N_K^+ - N_J)!} \left(\int_{xy} \tilde{j}_x^- \Delta_{xy}^R \tilde{j}_y^+ \right)^{P^+ - N_K^+ - N_J} \\ &\quad \times \frac{1}{(P^- - N_K^-)!} \left(\frac{1}{2} \int_{xy} \tilde{j}_x^- (2\Delta_{xy}^F - \Delta_{xy}^R - \Delta_{xy}^A) \tilde{j}_y^- \right)^{P^- - N_K^-}, \end{aligned} \quad (5.4)$$

where $N_K = N_K^+ + N_K^-$. Notice that the advanced contribution does not appear in the outgoing external legs since K_x acts only in the future of all other vertices.

If all of the external four-momenta are on-shell the purely on-shell combination $2\Delta_{xy}^F - \Delta_{xy}^R - \Delta_{xy}^A$ cannot occur in the internal lines of tree-level graphs by virtue of energy-momentum conservation. As such, we set $P^- = N_K^-$. Equation (5.4) then reduces to the following:

$$\begin{aligned} \Gamma_{JK}^{N_J \rightarrow N_K} &= (-1)^P 2^{1-N_K} g^V \frac{1}{V^+!} \left(\frac{1}{3!} \int_x (\tilde{\delta}_x^+)^3 \right)^{V^+} \frac{1}{V^-!} \left(\frac{1}{2!} \int_x (\tilde{\delta}_x^-)^2 \tilde{\delta}_x^+ \right)^{V^-} \\ &\quad \times \frac{1}{N_K!} \left(\int_{xy} K_x \Delta_{xy}^R \tilde{j}_y^+ \right)^{N_K^+} \left(\int_{xy} K_x (2\Delta_{xy}^F - \Delta_{xy}^R) \tilde{j}_y^- \right)^{N_K^-} \\ &\quad \times \frac{1}{N_J!} \left(\int_{xy} \tilde{j}_x^- \Delta_{xy}^R J_y \right)^{N_J} \frac{1}{(P - N)!} \left(\int_{xy} \tilde{j}_x^- \Delta_{xy}^R \tilde{j}_y^+ \right)^{P - N}. \end{aligned} \quad (5.5)$$

This is to be compared with the corresponding term in the expansion of the usual formula for the S-matrix:

$$S = : \exp \left[\int_x \phi_x^{\text{in}} (\square_x^2 + m^2) \delta_x \right] : \exp \left[\int_x \frac{g}{3!} \delta_x^3 \right] \exp \left[-\frac{1}{2} \int_{x,y} j_x \Delta_{xy}^F j_y \right] \Big|_{j=0}. \quad (5.6)$$

As in eq. (5.6), we can affect the LSZ reduction to map from the vacuum amplitude to the S-matrix by promoting the external sources to operators in Fock space, i.e.

$$\begin{aligned} K_x &\rightarrow \phi_x^{\text{out}} (\square_x^2 + m^2), \\ J_x &\rightarrow \phi_x^{\text{in}} (\square_x^2 + m^2). \end{aligned} \quad (5.7)$$

On contraction with the N_K -particle “out” and N_J -particle “in” Fock states, $\Gamma_{JK}^{N_J \rightarrow N_K}$ gives rise to a sum over all possible connected topologies. In the usual S-matrix approach, we would obtain a single graph for each topology. In the case of eq. (5.5) however, for each topology, we obtain a set of graphs with each graph contributing equally with a weight 2^{1-N_K} .

Comparing the remaining test sources and functional derivatives in eq. (5.5), the number of + type outgoing legs is given by

$$N_K^+ = P - 2V^+ = 2(N - V^+) - 3 \leq N_K. \quad (5.8)$$

Notice that, for ϕ^3 theory, N_K^+ is always odd. Thus the set of graphs consistent with a given topology corresponds to the sum over all ways of drawing that topology with an odd number of + type outgoing legs. The number of ways of arranging N_K^+ outgoing legs in a graph with a total of N_K outgoing legs is the binomial coefficient:

$$\frac{N_K!}{N_K^+!(N_K - N_K^+)!} = \frac{N_K!}{N_K^+!N_K^-!}. \quad (5.9)$$

The total number of graphs consistent with a given topology is then obtained by summing over all odd $1 \leq N_K^+ \leq N_K$, i.e.

$$\sum_{\substack{N_K^+ \geq 1 \\ \text{odd}}}^{N_K} \frac{N_K!}{N_K^+!(N_K - N_K^+)!} = 2^{N_K-1}. \quad (5.10)$$

This factor exactly cancels the overall factor of 2^{1-N_K} in Γ_{JK} and we are left with a sum over tree-level topologies, each with unit weight and entirely equivalent to the S-matrix result.

This equivalence with the S-matrix can be extended beyond tree-level. Specifically, a general retarded Green’s function ($\Gamma_{\text{R}}^{n \rightarrow m}$) can be obtained by summing over all circlings (see appendix A) except those of the m largest-time points, i.e.

$$\Gamma_{\text{R}}^{n \rightarrow m} = \Gamma_{\text{F}}^{n \rightarrow m} + \sum_{\text{circlings } \odot} \Gamma_{\odot}^{n \rightarrow m} \quad (5.11)$$

and we have isolated the zero-circlings contribution corresponding to a graph built entirely from Feynman propagators. Since the scattering amplitude $\Gamma_{JK}^{n \rightarrow m}$, derived in section 4, can be obtained from this retarded Green’s function after convoluting with the source/detector functions, it follows that the same $\Gamma_{JK}^{n \rightarrow m}$ could be obtained using the corresponding Feynman Green function, $\Gamma_{\text{F}}^{n \rightarrow m}$. This is because the second term on the right-hand side of

eq. (5.11) vanishes if we impose that the incoming particles carry positive energy forwards in time, which is the case when evaluating the S-matrix. At tree-level, we have just shown that the combinatoric factor associated with the convolution of the Green’s function and the sources is exactly as required for agreement with the S-matrix result, and this is sufficient to insure equivalence at all orders.

Note added: Whilst preparing the final version of this manuscript we became aware of reference [12], which presents a diagrammatic approach to the calculation of “in-in” expectation values similar to that presented in section 2 in the absence of external sources.

Acknowledgments

We should like to thank Ed Copeland, Fay Dowker, Tim Hollowood, Leif Lönnblad, Tim Morris, Mike Seymour and Graham Shore for many enjoyable and helpful discussions. We also thank Sean Carroll for provoking us in the first place. This work is partially supported by the Lancaster-Manchester-Sheffield Consortium for Fundamental Physics under STFC grant ST/J000418/1 and by the Royal Society. The work of PM is supported in part by the IPPP through STFC grant ST/G000905/1. PM would like to acknowledge the conferment of visiting researcher status at the University of Sheffield.

A Relation to unitarity cutting rules

We will now illustrate that the manifestly causal amplitudes derived from the operator and path-integral approaches are precisely the retarded amplitudes obtained by means of the Kobes-Semenoff unitarity cutting rules of the “in-in” formalism [13, 14]. For the purposes of this section, we will omit to write the physical sources and convolution integrals associated with the external propagators and we take the limits $T_A \rightarrow -\infty$, so that interaction vertices are integrated over an infinite domain.

We begin by noting the following diagrammatic representation of the time-ordered (Feynman), anti-time-ordered (Dyson) and Wightman propagators (e.g. see [15]):

$$\Delta_F(x, y) = \bullet \text{---} \diagup \text{---} \bullet \quad (\text{A.1a})$$

$$\Delta_D(x, y) = \textcircled{\bullet} \text{---} \diagup \text{---} \textcircled{\bullet} = \Delta_F^*(x, y) \quad (\text{A.1b})$$

$$-\Delta_>(x, y) = \textcircled{\bullet} \text{---} \diagup \text{---} \bullet = -\Delta_<^*(x, y) \quad (\text{A.1c})$$

$$-\Delta_<(x, y) = \bullet \text{---} \diagup \text{---} \textcircled{\bullet} . \quad (\text{A.1d})$$

We can follow the energy flow through a general graph built using these propagators since positive energy always flows from an uncircled into a circled vertex. The propagators satisfy

$$\bullet \text{---} \diagup \text{---} \bullet + \textcircled{\bullet} \text{---} \diagup \text{---} \textcircled{\bullet} + \textcircled{\bullet} \text{---} \diagup \text{---} \bullet + \bullet \text{---} \diagup \text{---} \textcircled{\bullet} = 0 . \quad (\text{A.2})$$

Notice that, unlike the usual unitarity cutting rules applied to S-matrix theory, the Kobes-Semenoff cutting rules do not restrict diagrams to contain only positive energy flow. As we shall see below, negative energy flow is necessary for the construction of retarded diagrams and the restoration of manifest causality.

In terms of the propagators above, the retarded propagator can be expressed as

$$\begin{aligned}
\Delta_{\text{R}}(x, y) &\equiv \bullet \text{---} \bullet = \bullet \text{---} \diagup \bullet + \bullet \text{---} \diagup \odot \\
&= - \odot \text{---} \diagup \odot - \odot \text{---} \diagup \bullet \\
&= \odot \text{---} \odot \\
&= - \bullet \text{---} \odot = - \odot \text{---} \bullet . \tag{A.3}
\end{aligned}$$

In other words, circling plays no role for retarded propagators except to help keep track of the minus signs.

By virtue of the Kobes-Semenoff cutting rules, the one-loop, negative-frequency Wightman propagator is obtained by circling the right-most external vertex and summing over all possible circlings of the internal vertices. The one-loop retarded propagator then takes the form

$$\begin{aligned}
\Delta_{\text{R}}^{(1)}(x, y) &= \Delta_{\text{F}}^{(1)}(x, y) - \Delta_{<}^{(1)}(x, y) \\
&= \bullet \text{---} \diagup \bullet + \bullet \text{---} \diagup \odot \\
&+ \bullet \text{---} \diagup \bullet \text{---} \text{---} \bullet \\
&+ \bullet \text{---} \diagup \bullet \text{---} \text{---} \odot + \bullet \text{---} \diagup \bullet \text{---} \text{---} \odot \\
&+ \bullet \text{---} \diagup \odot \text{---} \text{---} \odot + \bullet \text{---} \diagup \odot \text{---} \text{---} \odot . \tag{A.4}
\end{aligned}$$

Since energy is conserved through the internal vertices the following circlings are identically zero:

$$\bullet \text{---} \diagup \odot \text{---} \text{---} \bullet = \bullet \text{---} \diagup \bullet \text{---} \text{---} \odot = \bullet \text{---} \diagup \bullet \text{---} \text{---} \odot = 0 . \tag{A.5}$$

Notice that the last diagram in eq. (A.4) is also vanishing. Adding to eq. (A.4) the vanishing diagrams from eq. (A.5), we make the following observation: the retarded diagram is obtained by summing over all possible circlings of vertices whilst leaving the outgoing, leftmost point uncircled [6].

The one-loop contribution then contains 8 diagrams:

$$\begin{aligned}
\Delta_{\text{R}}^{(\delta 1)}(x, y) = & \text{Diagram 1} + \text{Diagram 2} \\
& + \text{Diagram 3} + \text{Diagram 4} \\
& + \text{Diagram 5} + \text{Diagram 6} \\
& + \text{Diagram 7} + \text{Diagram 8}, \tag{A.6}
\end{aligned}$$

where $\Delta_{\text{R}}^{(\delta 1)}(x, y) = \Delta_{\text{R}}^{(1)}(x, y) - \Delta_{\text{R}}(x, y)$. Combining each pair of diagrams row by row in eq. (A.6), using the identities in eq. (A.3), we obtain

$$\begin{aligned}
\Delta_{\text{R}}^{(\delta 1)}(x, y) = & \text{Diagram 1} + \text{Diagram 2} \\
& + \text{Diagram 3} + \text{Diagram 4}. \tag{A.7}
\end{aligned}$$

Splitting the remaining diagrams into their component parts, we may write

$$\begin{aligned}
\Delta_{\text{R}}^{(\delta 1)}(x, y) = & \text{Diagram 1} \left[\text{Diagram 5} - \text{Diagram 6} \right] \\
& + \text{Diagram 2} \left[\text{Diagram 7} - \text{Diagram 8} \right]. \tag{A.8}
\end{aligned}$$

Again using the identities in eq. (A.3), this may recast in terms of Feynman and retarded propagators as

$$\Delta_{\text{R}}^{(\delta 1)}(x, y) = \text{Diagram 1} \left[2 \text{Diagram 5} - \text{Diagram 6} \right]. \tag{A.9}$$

Finally, after recombining the component pieces, we arrive at the one-loop retarded propagator

$$\Delta_{\text{R}}^{(1)}(x, y) = \text{Diagram 1} + 2 \text{Diagram 2} - \text{Diagram 3} \tag{A.10}$$

which is of precisely the expected form, i.e.

$$\Delta_{\text{R}}^{(1)}(x, y) = \Delta_{\text{R}}(x, y) + \Delta_{\text{R}}(x, z) \star \Pi_{\text{R}}^{(1)}(z, z') \star \Delta_{\text{R}}(z', y), \quad (\text{A.11})$$

where

$$\Pi_{\text{R}}^{(1)}(z, z') = \frac{(-ig)^2}{2!} \left[2\Delta_{\text{F}}(z, z')\Delta_{\text{R}}(z, z') - (\Delta_{\text{R}}(z, z'))^2 \right] \quad (\text{A.12})$$

is the truncated one-loop retarded self energy and \star denotes integration over the intermediate spacetime points z and z' .

It is interesting to see how this works starting from the truncated self-energy. In terms of the Kobes-Semenoff cutting rules, this is

$$\begin{aligned} \Pi_{\text{R}}^{(1)}(z, z') &= \Pi^{(1)}(z, z') - \Pi_{<}^{(1)}(z, z') = \frac{(-ig)^2}{2!} \left[(\Delta_{\text{F}}(z, z'))^2 - (\Delta_{<}(z, z'))^2 \right] \\ &= \text{[Diagram 1]} + \text{[Diagram 2]}. \end{aligned} \quad (\text{A.13})$$

Proceeding as before by separating the truncated self-energy into its component parts, we obtain

$$\Pi_{\text{R}}^{(1)}(z, z') = \bullet \left[\text{[Diagram 3]} - \text{[Diagram 4]} \right] \bullet. \quad (\text{A.14})$$

Substituting the decomposition of the retarded propagator from eq. (A.3), this may be written in terms of only Feynman and retarded propagators exactly as before, i.e.

$$\Pi_{\text{R}}^{(1)}(z, z') = 2 \text{[Diagram 5]} - \text{[Diagram 6]}. \quad (\text{A.15})$$

Following the same circling rules for the one-to-two scattering, i.e. we do not circle the ‘‘latest time’’ vertices that we anticipate coupling to detector sources K , the retarded contribution to the time-ordered 3-point function is given by

$$\begin{aligned} \Gamma_{\text{R}}^{1 \rightarrow 2}(x, y, z) &= \text{[Diagram 7]} + \text{[Diagram 8]} + \text{[Diagram 9]} + \text{[Diagram 10]} \\ &= \text{[Diagram 11]} + \text{[Diagram 12]}. \end{aligned} \quad (\text{A.16})$$

Separating the component contributions, we have

$$\Gamma_{\text{R}}^{1 \rightarrow 2}(x, y, z) = \left[\text{[Diagram 13]} - \text{[Diagram 14]} \right] \bullet \text{---} \bullet, \quad (\text{A.17})$$

yielding

$$\Gamma_{\text{R}}^{1 \rightarrow 2}(x, y, z) = \begin{array}{c} \bullet \\ \diagdown \\ \bullet \\ \diagup \\ \bullet \end{array} \text{---} \bullet + \begin{array}{c} \bullet \\ \diagup \\ \bullet \\ \diagdown \\ \bullet \end{array} \text{---} \bullet - \begin{array}{c} \bullet \\ \diagdown \\ \bullet \\ \diagup \\ \bullet \end{array} \text{---} \bullet, \quad (\text{A.18})$$

which is in agreement with eq. (4.34) after convoluting with the source functions.

We may repeat this diagrammatic manipulation for two-to-two scattering, which corresponds to 16 circlings:

$$\Gamma_{\text{R}}^{2 \rightarrow 2}(x, y, z, w) = \begin{array}{cccc} \begin{array}{c} \bullet \\ \diagdown \\ \bullet \\ \diagup \\ \bullet \end{array} \text{---} \begin{array}{c} \bullet \\ \diagup \\ \bullet \\ \diagdown \\ \bullet \end{array} & + & \begin{array}{c} \bullet \\ \diagup \\ \bullet \\ \diagdown \\ \bullet \end{array} \text{---} \begin{array}{c} \bullet \\ \diagdown \\ \bullet \\ \diagup \\ \bullet \end{array} & + & \begin{array}{c} \bullet \\ \diagdown \\ \bullet \\ \diagup \\ \bullet \end{array} \text{---} \begin{array}{c} \bullet \\ \diagup \\ \bullet \\ \diagdown \\ \bullet \end{array} & + & \begin{array}{c} \bullet \\ \diagup \\ \bullet \\ \diagdown \\ \bullet \end{array} \text{---} \begin{array}{c} \bullet \\ \diagdown \\ \bullet \\ \diagup \\ \bullet \end{array} \\ \begin{array}{c} \bullet \\ \diagdown \\ \bullet \\ \diagup \\ \bullet \end{array} \text{---} \begin{array}{c} \bullet \\ \diagup \\ \bullet \\ \diagdown \\ \bullet \end{array} & + & \begin{array}{c} \bullet \\ \diagup \\ \bullet \\ \diagdown \\ \bullet \end{array} \text{---} \begin{array}{c} \bullet \\ \diagdown \\ \bullet \\ \diagup \\ \bullet \end{array} & + & \begin{array}{c} \bullet \\ \diagdown \\ \bullet \\ \diagup \\ \bullet \end{array} \text{---} \begin{array}{c} \bullet \\ \diagup \\ \bullet \\ \diagdown \\ \bullet \end{array} & + & \begin{array}{c} \bullet \\ \diagup \\ \bullet \\ \diagdown \\ \bullet \end{array} \text{---} \begin{array}{c} \bullet \\ \diagdown \\ \bullet \\ \diagup \\ \bullet \end{array} \\ \begin{array}{c} \bullet \\ \diagdown \\ \bullet \\ \diagup \\ \bullet \end{array} \text{---} \begin{array}{c} \bullet \\ \diagup \\ \bullet \\ \diagdown \\ \bullet \end{array} & + & \begin{array}{c} \bullet \\ \diagup \\ \bullet \\ \diagdown \\ \bullet \end{array} \text{---} \begin{array}{c} \bullet \\ \diagdown \\ \bullet \\ \diagup \\ \bullet \end{array} & + & \begin{array}{c} \bullet \\ \diagdown \\ \bullet \\ \diagup \\ \bullet \end{array} \text{---} \begin{array}{c} \bullet \\ \diagup \\ \bullet \\ \diagdown \\ \bullet \end{array} & + & \begin{array}{c} \bullet \\ \diagup \\ \bullet \\ \diagdown \\ \bullet \end{array} \text{---} \begin{array}{c} \bullet \\ \diagdown \\ \bullet \\ \diagup \\ \bullet \end{array} \\ \begin{array}{c} \bullet \\ \diagdown \\ \bullet \\ \diagup \\ \bullet \end{array} \text{---} \begin{array}{c} \bullet \\ \diagup \\ \bullet \\ \diagdown \\ \bullet \end{array} & + & \begin{array}{c} \bullet \\ \diagup \\ \bullet \\ \diagdown \\ \bullet \end{array} \text{---} \begin{array}{c} \bullet \\ \diagdown \\ \bullet \\ \diagup \\ \bullet \end{array} & + & \begin{array}{c} \bullet \\ \diagdown \\ \bullet \\ \diagup \\ \bullet \end{array} \text{---} \begin{array}{c} \bullet \\ \diagup \\ \bullet \\ \diagdown \\ \bullet \end{array} & + & \begin{array}{c} \bullet \\ \diagup \\ \bullet \\ \diagdown \\ \bullet \end{array} \text{---} \begin{array}{c} \bullet \\ \diagdown \\ \bullet \\ \diagup \\ \bullet \end{array} \end{array}. \quad (\text{A.19})$$

After pairwise contracting the diagrams and expanding the component propagators by means of eq. (A.3), we may show that these 16 ordered diagrams reduce to the following three diagrams:

$$\Gamma_{\text{R}}^{2 \rightarrow 2}(x, y, z, w) = \begin{array}{c} \bullet \\ \diagdown \\ \bullet \\ \diagup \\ \bullet \end{array} \text{---} \begin{array}{c} \bullet \\ \diagup \\ \bullet \\ \diagdown \\ \bullet \end{array} + \begin{array}{c} \bullet \\ \diagup \\ \bullet \\ \diagdown \\ \bullet \end{array} \text{---} \begin{array}{c} \bullet \\ \diagdown \\ \bullet \\ \diagup \\ \bullet \end{array} - \begin{array}{c} \bullet \\ \diagdown \\ \bullet \\ \diagup \\ \bullet \end{array} \text{---} \begin{array}{c} \bullet \\ \diagup \\ \bullet \\ \diagdown \\ \bullet \end{array}, \quad (\text{A.20})$$

again in agreement with the earlier results (see the sentence below eq. (3.13)). The results of this section serve to illustrate the role played by negative energy flow forwards in time in building causal amplitudes.

B Propagator definitions

Here we collect together the definitions of the various propagators that appear.

- The Wightman propagators:

$$\begin{aligned} \Delta_{>}(x, y) &= \langle \phi(x)\phi(y) \rangle = \int \frac{d^3\mathbf{p}}{(2\pi)^3 2E} e^{-ip \cdot (x-y)} \\ &= \int \frac{d^4p}{(2\pi)^3} \delta(p^2 - m^2) \Theta(p_0) e^{-ip \cdot (x-y)}, \end{aligned} \quad (\text{B.1})$$

$$\begin{aligned}
\Delta_{<}(x, y) &= \langle \phi(y)\phi(x) \rangle = \int \frac{d^3\mathbf{p}}{(2\pi)^3 2E} e^{+ip \cdot (x-y)} \\
&= \int \frac{d^4p}{(2\pi)^3} \delta(p^2 - m^2) \Theta(-p_0) e^{-ip \cdot (x-y)} .
\end{aligned} \tag{B.2}$$

- The Pauli-Jordan propagator, $\Delta(x, y) = \Delta_{>}(x, y) - \Delta_{<}(x, y)$:

$$\Delta(x, y) = \Delta_{yx} = \langle [\phi(x), \phi(y)] \rangle = \int \frac{d^3\mathbf{p}}{(2\pi)^3 2E} \left(e^{-ip \cdot (x-y)} - e^{+ip \cdot (x-y)} \right) . \tag{B.3}$$

- The Hadamard propagator, $\Delta_1(x, y) = \Delta_{>}(x, y) + \Delta_{<}(x, y)$:

$$\Delta_1(x, y) = \langle \{\phi(x), \phi(y)\} \rangle = \int \frac{d^3\mathbf{p}}{(2\pi)^3 2E} \left(e^{-ip \cdot (x-y)} + e^{+ip \cdot (x-y)} \right) . \tag{B.4}$$

- The Feynman and Dyson propagators, $\Delta_F(x, y) = \Delta_D^*(x, y)$:

$$\begin{aligned}
\Delta_F(x, y) &= \langle T[\phi(x)\phi(y)] \rangle = \Delta_{>}(x, y)\Theta(x^0 - y^0) + \Delta_{<}(x, y)\Theta(y^0 - x^0) \\
&= \int \frac{d^4k}{(2\pi)^4} e^{-ik \cdot (x-y)} \frac{i}{k^2 - m^2 + i\epsilon} \\
&= i \int \frac{d^4k}{(2\pi)^4} e^{-ik \cdot (x-y)} \left[P \left(\frac{1}{k^2 - m^2} \right) - i\pi\delta(k^2 - m^2) \right]
\end{aligned} \tag{B.5}$$

where P denotes the Cauchy Principal Value.

- The retarded and advanced propagators, $\Delta_R(x, y) = \Delta_A(y, x)$:

$$\begin{aligned}
\Delta_R(x, y) &= \Delta(x, y)\Theta(x^0 - y^0) \\
&= \int \frac{d^4k}{(2\pi)^4} e^{-ik \cdot (x-y)} \frac{i}{(k_0 + i\epsilon)^2 - \mathbf{k}^2 - m^2} \\
&= i \int \frac{d^4k}{(2\pi)^4} e^{-ik \cdot (x-y)} \left[P \left(\frac{1}{k^2 - m^2} \right) - i\pi\delta(k^2 - m^2)\text{sgn}(k_0) \right] .
\end{aligned} \tag{B.6}$$

References

- [1] J. D. Franson and M. M. Donegan, *Perturbation theory for quantum-mechanical observables*, *Phys. Rev. A* **65** (2002), no. 5 052107.
- [2] M. K. Transtrum and J.-F. S. Van Huele, *Commutation relations for functions of operators*, *Journal of Mathematical Physics* **46** (2005) 063510.
- [3] J. S. Schwinger, *Brownian motion of a quantum oscillator*, *J. Math. Phys.* **2** (1961) 407–432.
- [4] L. Keldysh, *Diagram technique for nonequilibrium processes*, *Zh. Eksp. Teor. Fiz.* **47** (1964) 1515–1527.
- [5] P. Millington and A. Pilaftsis, *Perturbative non-equilibrium thermal field theory*, *Phys. Rev. D* **88** (2013) 085009, [[arXiv:1211.3152](https://arxiv.org/abs/1211.3152)].
- [6] R. Kobes, *Retarded functions, dispersion relations, and Cutkosky rules at zero and finite temperature*, *Phys. Rev. D* **43** (1991) 1269–1282.

- [7] M. van Eijck and C. van Weert, *Finite temperature retarded and advanced Green functions*, *Phys. Lett. B* **278** (1992) 305–310.
- [8] E. Calzetta and B. L. Hu, *Nonequilibrium quantum fields: closed time path effective action, Wigner function and Boltzmann equation*, *Phys. Rev. D* **37** (1988) 2878–2900.
- [9] E. Calzetta and B. L. Hu, *Closed time path functional formalism in curved spacetime: application to cosmological back-reaction problems*, *Phys. Rev. D* **35** (1987) 495–509.
- [10] R. Jordan, *Effective field equations for expectation values*, *Phys.Rev.* **D33** (1986) 444–454.
- [11] M. A. van Eijck, R. Kobes, and C. G. van Weert, *Transformations of real-time finite-temperature Feynman rules*, *Phys. Rev. D* **50** (1994) 4097–4109, [[hep-ph/9406214](#)].
- [12] M. Musso, *A new diagrammatic representation for correlation functions in the in-in formalism*, *JHEP* **1311** (2013) 184, [[hep-th/0611258](#)].
- [13] R. Kobes and G. Semenoff, *Discontinuities of Green Functions in Field Theory at Finite Temperature and Density*, *Nucl. Phys. B* **260** (1985) 714–746.
- [14] R. Kobes and G. Semenoff, *Discontinuities of Green Functions in Field Theory at Finite Temperature and Density. 2*, *Nucl. Phys. B* **272** (1986) 329–364.
- [15] M. Veltman, *Diagrammatica: the path to Feynman rules*. Cambridge University Press, Cambridge U.K., 1994.